JACS
JOURNAL OF THE AMERICAN CHEMICAL SOCIETY
Communication
pubs.acs.org/JACS

Beyond Platinum: Bubble-Propelled Micromotors Based on Ag and MnO_2 Catalysts

Hong Wang, Guanjia Zhao, and Martin Pumera*

Division of Chemistry & Biological Chemistry, School of Physical and Mathematical Sciences, Nanyang Technological University, Singapore 637371, Singapore

Web-Enhanced Feature Supporting Information

ABSTRACT: Autonomous bubble-propelled catalytic micro- and nanomachines show great promise in the fields of biomedicine, environmental science, and natural resources. It is envisioned that thousands and millions of such micromachines will swarm and communicate with each other, performing desired actions. To date, mainly platinum catalyst surfaces have been used for the decomposition of a fuel, hydrogen peroxide, to oxygen bubbles. Here we propose Pt-free, low-cost inorganic catalysts for powering micromotors based on silver and manganese dioxide surfaces. Such Ag- and MnO_2-based bubble-powered micromotors show fast motion even at very low concentrations of fuel, down to 0.1% of H_2O_2. These catalysts should enable unparalleled widespread use of such motors in real applications, as it will be possible to make them in large quantities at low cost.

Self-propelled autonomous micromotors and micromachines are at the forefront of research in micro- and nanotechnology.[1−6] These autonomous devices have the potential to play vital roles in drug delivery,[7−9] microsurgery,[10,11] environmental remediation,[12−14] and natural resources discovery.[15,16]

There are three types of mechanisms describing the motion of catalytic micro-/nanomotors: (i) self-diffusiophoresis,[17] (ii) self-electrophoresis,[18] and (iii) bubble ejection.[19] Devices relying on (i) self-diffusiophoresis propulsion decompose asymmetrically the fuel presented in their environment.[20,21] They move in the direction of the self-generated concentration gradient in their vicinity. The motion of micromotors propelled by self-diffusiophoresis does not involve bubble generation, and the micromotors generally exhibit slow motion.[22] (ii) Self-electrophoretic micromotors rely on the simultaneous oxidation and reduction of fuel at the opposite ends of the device. Such redox reactions lead to the flow of the electrons across the device, which is accompanied by a flow of hydronium ions at the surface of the microdevice and consequent propulsion.[23] (iii) A bubble-propulsion mechanism for powering micromotors has become highly popular in recent years.[24−26] Decomposition of hydrogen peroxide over a catalytic surface, such as platinum, creates bubbles and propels the micromotor forward.[19] The advantages of this mechanism are its high power output, its robust performance, and the very high speed the devices can achieve, dramatically overcoming the velocity of the devices powered by mechanisms (i) and (ii).

To date, despite tens of articles published in the field of bubble-propelled micro-/nanomotors, the vast majority of bubble-powered micromotors have used Pt as catalyst,[25,27,28] with only a few exceptions. A Communication by Sanchez et al. showed the utility of an enzyme to decompose H_2O_2.[29] While the use of enzymes shows ingenuity, the disadvantage is their limited lifetime. Complex Ti/Fe/Au/Ag nanomembrane microjet motors were also produced previously.[30] Given the significant cost of Pt as catalyst and/or nanomachining as fabrication method, we wish to demonstrate that simple and widely available inorganic materials can be used for bubble-propelled motors. We will demonstrate that simple silver and managnese dioxide particles are highly efficient to decompose H_2O_2 fuel, leading to fast bubble-propelled motion of micromotors. The use of Ag and MnO_2 as potential candidate materials for micromotor fabrication is very attractive because of the excellent catalytic properties, low costs, low concentration of fuel needed, high efficiency, and long lifetime.

First we discuss the silver-surface-catalyzed bubble-propelled micromotors. Figure 1A shows time-lapse images of the movement of a Ag micromotor in 9% H_2O_2 (see also Video 1). Figure S-1 (Supporting Information) shows a tracking image for the path of a Ag catalytic micromotor in 0.5% H_2O_2 over a 2 s time interval. Oxygen bubbles are generated by the catalytic decomposition of H_2O_2 by Ag, and they are released from one side of the motor. Asymmetry is the key to the design of micro-/nanomotors. For spherical Janus motors, the motion is usually attributed to asymmetric generation of bubbles achieved by a partial inert coating, without which no directional movement is achieved due to expected lack of asymmetric bubble thrust.[1,20] However, the Ag micromotors used here feature inhomogeneity and asymmetry. Bubble generation is closely related to the geometry of the motors, and bubble nucleation on solid surface needs gases to reach heterogeneous nucleation energy, which depends on the gas saturation concentration and the curvature of the surface. Less energy is required for bubble formation on a flat surface than on a convex surface, and even less energy is required on a concave surface.[31,32] We have conducted experiments in which Ag micromotors were half-covered with Au using sputtering, but little difference in mobility was observed compared to the unsputtered ones, showing that the bubble generation is more related to the instinctive morphology of the particles. Three typical kinds of trajectories were found for the motion of the Ag

Received: November 17, 2013
Published: February 7, 2014

   dx.doi.org/10.1021/ja411705d | J. Am. Chem. Soc. 2014, 136, 2719−2722

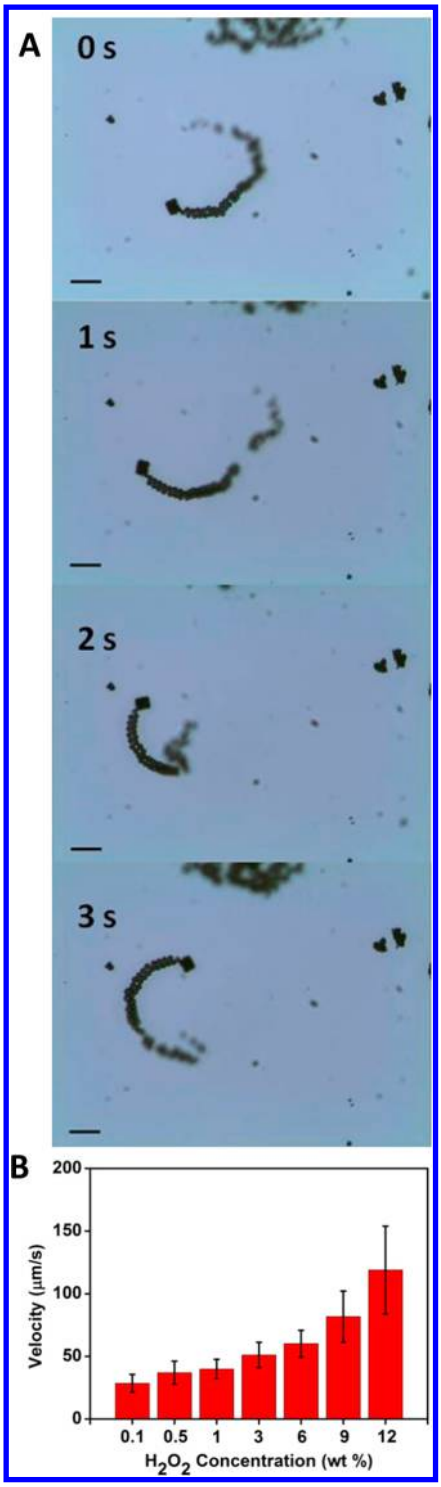

Figure 1. Motion of silver catalytic micromotors. (A) Time-lapse images of a Ag micromotor in 9% H_2O_2 and 0.5% SDS solution (scale bar = 50 μm). (B) Dependence of the average velocity of Ag catalytic micromotors on H_2O_2 concentration at 23 °C. Video 1 shows the moving Ag micromotor motor in 9% H_2O_2.

catalytic micromotors: circular, curved, and self-rotating motions. The different trajectories derive from the differences in size, shape, and geometry of the catalytic micromotor, similar to the case of tubular micromotors.[24]

The velocity of the Ag catalytic motor is dependent on the H_2O_2 fuel concentration. Figure 1B illustrates the influence of H_2O_2 concentration on the average speed of the moving Ag micromotors (see also Figure S-2 for velocity expressed in body lengths per second; the size of the particular micromotor shown in Figure 1A is 20 μm). As expected, Ag micromotors show clearly increased velocities with increasing fuel concentration. The percentage of Ag motors exhibiting motion among all the Ag particles and the mobility of the motors depend on the fuel concentration and instinctive morphology of the Ag particles.

There is an obvious increase in the mobility of Ag micromotors with increasing concentration of H_2O_2. Due to the propulsion by vigorous bubbling, the mobility of the Ag catalytic motor is quite high compared to that of the Pt catalytic Janus motors that move by diffusiophoresis, reported previously.[33−35] Silver micromotors can move at an average speed of ∼25 μm/s, even in 0.1% H_2O_2, and the average speed of Ag catalytic motors exhibiting motion can reach over 100 μm/s in the presence of 12% H_2O_2. The high bubble frequency reflects the high catalytic efficiency of Ag for the decomposition of H_2O_2. Given the low costs and good performance, Ag is a promising candidate catalyst for preparation of micro-/nanomotors. However, it should be noted that, with decreasing amount of fuel, the percentage of motors exhibiting motion decreases, as shown in Figure S-3.

Manganese dioxide is another well-known catalyst that can accelerate the decomposition of H_2O_2, and it is much cheaper and more accessible than the noble metal often used in the preparation of micro-/nanomotors. MnO_2 is widely used in industry for cheap carbon/MnO_2 batteries.[36] Next we investigate the motion of micromotors based on MnO_2 microparticles in H_2O_2 solution. Similar to Ag particles, MnO_2 micromotors exhibit motion propelled by oxygen bubbles. However, the proportion of moving MnO_2 micromotors is much less than that for Ag particles, and higher concentrations of H_2O_2 are needed for efficient propulsion. Figure 2A shows time-lapse frames from a video of MnO_2 micromotors in 15% H_2O_2. The size of the particular micromotor in Figure 2A is 5 μm. Figure S-4 tracks a MnO_2 motor in the presence of 21% H_2O_2 for 2 s (see also Videos 2 and 3). As illustrated in Figure 2B, the average speed of moving MnO_2 micromotors increases from ∼50 μm/s at 12% H_2O_2 to ∼120 μm/s at 21% H_2O_2 (see Figure S-5 for velocity expressed in body lengths/s). The proportion of MnO_2 micromotors exhibiting motion also decreases with decreasing H_2O_2 concentration. Nevertheless, the excellent mobility of MnO_2 micromotors demonstrates the potential of MnO_2 to be involved in the preparation of micro-/nanomotors if modified to proper morphology.

Various control experiments, illustrated in Figure 3, were used to confirm the propulsion by oxygen bubbles generated by catalytic decomposition of H_2O_2. No bubble generation was observed for MoO_2 and MoO_3 in the presence of 21% H_2O_2 and 0.5% sodium dodecyl sulfate (SDS) due to the absence of catalytic property of molybdenum oxides. Similarly, no bubble propulsion was observed for MnO_2 and Ag particles in the absence of H_2O_2. In contrast, the mobility of MnO_2 and Ag particles in H_2O_2 reflects the efficient bubble propulsion associated with their good catalytic properties. The mean square displacement (MSD) of Ag and MnO_2 motors showed a parabolic dependence on time (Figures S-6 and S-7, respectively), which indicates that the motion is driven by bubble ejection instead of Brownian motion.[33,37] The efficiency of the Ag motor in 9% H_2O_2 was found to be 5.81×10^{-8}, while the efficiency of the MnO_2 motor in 12% H_2O_2 was 1.16

dx.doi.org/10.1021/ja411705d | J. Am. Chem. Soc. 2014, 136, 2719−2722

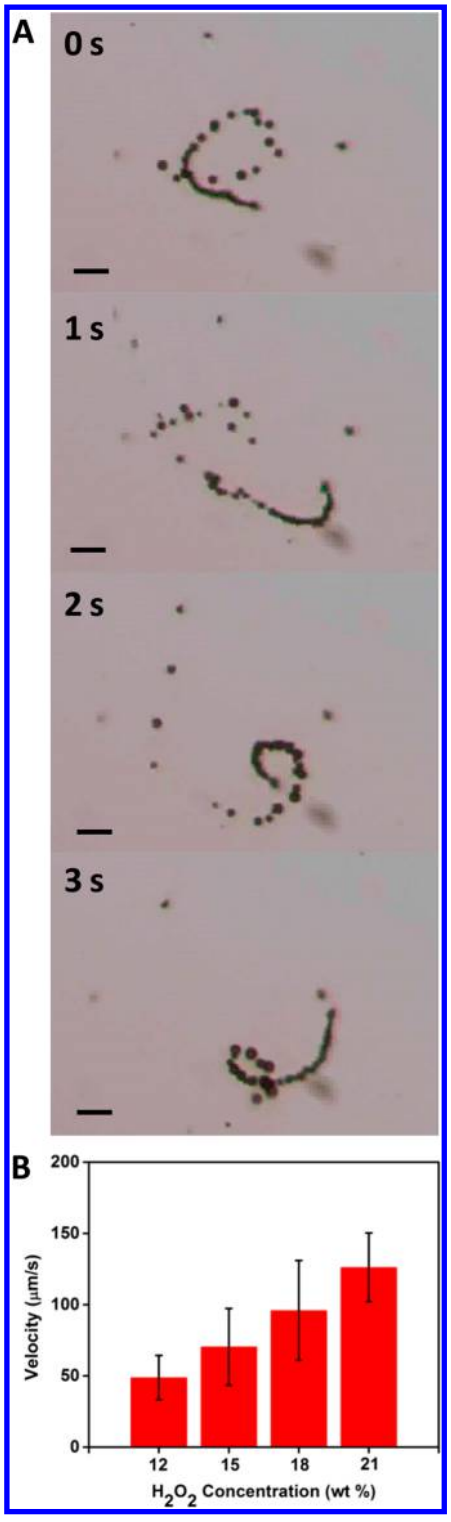

Figure 2. Motion of manganese dioxide catalytic micromotors. (A) Time-lapse images of a MnO_2 catalytic micromotor in 15% H_2O_2 and 0.5% SDS solution (scale bar = 20 μm). (B) Dependence of the average velocity of MnO_2 catalytic micromotors on H_2O_2 concentration at 23 °C. Video 2 shows the moving 5 μm MnO_2 micromotor in 15% H_2O_2. Similarly, Video 3 tracks a MnO_2 micromotor in the presence of 21% H_2O_2 (see Figure S-4).

$\times 10^{-8}$, following the calculation approach previously reported (see Supporting Information for details).[38] This compares favorably with previously established efficiencies of other Janus particles that move by diffusiophoresis (efficiency = 5×10^{-10})

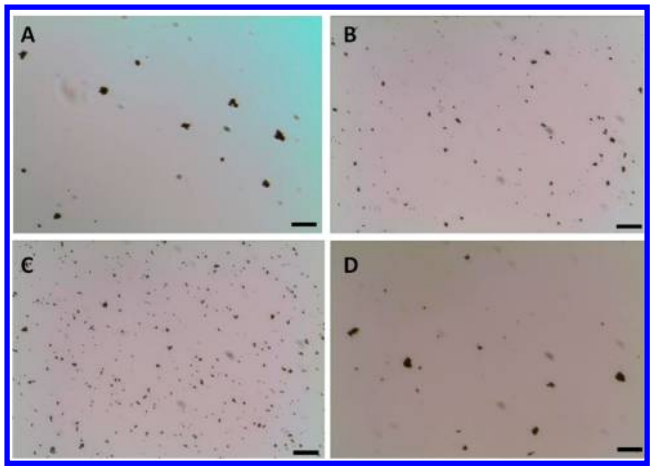

Figure 3. Control experiments: (A) Ag and (B) MnO_2 particles in 0.5% SDS solution and (C) MoO_3 and (D) MoO_2 particles in 21% H_2O_2 and 0.5% SDS solution (scale bars = 50 μm). Conditions: temperature, 23 °C; particle concentration, 1 mg/mL.

and bubble-propelled tubular microjets (efficiency = 2.4×10^{-10}).[38]

An advantage of Ag and MnO_2 materials over Pt is that they are much less prone to poisoning. It has been previously demonstrated that Pt catalytic bubble-propelled microjet engines are susceptible to thiol poisoning, even at micromolar concentration of thiols.[39] We compared the motion of Ag motors in 3% H_2O_2 without and with addition of 10 mM cysteine. No observable difference in the velocity of the Ag motors was found. Similarly, MnO_2 is not prone to thiol poisoning. It should be mentioned that the micromotors reported here are truly catalytic, and their motion stops only when the fuel is exhausted. When fuel is replenished, the bubble-propelled motion of the micromotors resumes, and the micromotors move over the span of the whole experiment with the same agility.

In summary, we have presented new materials for catalytic propulsion of bubble-powered micromotors, silver and manganese dioxide. These Pt-free, Ag- and MnO_2-based micromotors, driven by the bubbles from catalytic decomposition of hydrogen peroxide, exhibited fast motion. The speed of the micromotors can be modulated by changing the concentration of H_2O_2, and efficient propulsion can be achieved even at very low concentration (0.1%) of H_2O_2 fuel. The low costs, high efficiency, and good stability of Ag and MnO_2 (compared to Mg- and Al-based micromotors[12,40,41]) make them attractive alternatives to the currently popular platinum for prolonged propulsion of micro-/nanomotors in diverse ranges of practical applications. Additional efforts should be devoted to further functionalization and modification of Ag and MnO_2 micromotors for applications in biomedical and environmental fields. It is envisioned that such accessible and affordable inorganic materials will replace the need for Pt in these artificial organisms and contribute to their fabrication in millions and millions of copies.

■ ASSOCIATED CONTENT

Ⓢ Supporting Information

Experimental details, tracking of Ag and MnO_2 micromotors, plots of velocities of Ag and MnO_2 micromotors in body lengths/s, MSD analysis, and SEM images. This material is available free of charge via the Internet at http://pubs.acs.org.

dx.doi.org/10.1021/ja411705d | J. Am. Chem. Soc. 2014, 136, 2719−2722

Web-Enhanced Feature

Videos 1−3 in .avi format are available in the online versions of the paper.

AUTHOR INFORMATION

Corresponding Author

pumera@ntu.edu.sg

Notes

The authors declare no competing financial interest.

ACKNOWLEDGMENTS

M.P. thanks NAP for funding (NTU).

REFERENCES

(1) Paxton, W. F.; Sundararajan, S.; Mallouk, T. E.; Sen, A. *Angew. Chem., Int. Ed.* **2006**, *45*, 5420.
(2) Sanchez, S.; Pumera, M. *Chem.−Asian J* **2009**, *4*, 1402.
(3) Fisher, P.; Ghosh, A. *Nanoscale* **2011**, *3*, 557.
(4) Sengupta, S.; Ibele, M.; Sen, A. *Angew. Chem., Int. Ed.* **2012**, *51*, 8434.
(5) Wang, J. *ACS Nano* **2009**, *3*, 4.
(6) Mei, Y. F.; Solovev, A. A.; Sanchez, S.; Schmidt, O. G. *Chem. Soc. Rev.* **2011**, *40*, 2109.
(7) Wu, Y.; Wu, Z.; Lin, X.; He, Q.; Li, J. *ACS Nano* **2012**, *6*, 10910.
(8) Wu, Z.; Wu, Y.; He, W.; Lin, X.; Sun, J.; He, Q. *Angew. Chem., Int. Ed.* **2013**, *52*, 7000.
(9) Kagan, D.; Laocharoensuk, R.; Zimmerman, M.; Clawson, C.; Balasubramanian, S.; Kang, D.; Bishop, D.; Sattayasamitsathit, S.; Zhang, L.; Wang, J. *Small* **2010**, *6*, 2741.
(10) Kagan, D.; Benchimol, M. J.; Claussen, J. C.; Chuluun-Erdene, E.; Esener, S.; Wang, J. *Angew. Chem., Int. Ed.* **2012**, *30*, 7519.
(11) Solovev, A. A.; Xi, W.; Gracias, D. H.; Harazim, S. M.; Deneke, D.; Sanchez, S.; Schmidt, O. G. *ACS Nano* **2012**, *6*, 1751.
(12) Gao, W.; Feng, X.; Pei, A.; Gu, Y.; Li, J.; Wang, J. *Nanosacle* **2013**, *5*, 4696.
(13) Soler, L.; Magdanz, V.; Fomin, V. M.; Sanchez, S.; Schmidt, O. G. *ACS Nano* **2013**, *7*, 9611.
(14) Orozco, J.; Cheng, G.; Vilela, D.; Sattayasamitsathit, S.; Duhalt, G. V.; Pak, O. S.; Escarpa, A.; Kan, C.; Wang, J. *Angew. Chem., Int. Ed.* **2013**, *52*, 13276.
(15) Orozco, J.; García-Gradilla, V.; D'Agostino, M.; Gao, W.; Cortés, A.; Wang, J. *ACS Nano* **2013**, *7*, 818.
(16) Zhao, G.; Wang, H.; Khezri, B.; Wester, R. D.; Pumera, M. *Lab Chip* **2013**, *13*, 2937.
(17) Popescu, M. N.; Dietrich, S.; Tasinkevych, M.; Ralston, J. *Eur. Phys. J. E* **2010**, *31*, 351.
(18) Wang, Y.; Hernandez, R. M.; Bartlett, D. J.; Bingham, J. M., Jr.; Kline, T. R.; Sen, A.; Mallouk, T. E. *Langmuir* **2006**, *22*, 10451.
(19) Solovev, A. A.; Sanchez, S.; Pumera, M.; Mei, Y. F.; Schmidt, O. G. *Adv. Funct. Mater.* **2010**, *20*, 2430.
(20) Gao, W.; D'Agostino, M.; Garcia-Gradilla, V.; Orozco, J.; Wang, J. *Small* **2013**, *9*, 467.
(21) Muddana, H. S.; Sengupta, S.; Mallouk, T. E.; Sen, A.; Butler, P. J. *J. Am. Chem. Soc.* **2010**, *132*, 2210.
(22) Paxton, W. F.; Kistler, K. C.; Olmeda, C. C.; Sen, A.; St. Angelo, S. K.; Cao, Y.; Mallouk, T.; Lammert, P. E.; Crespi, V. H. *J. Am. Chem. Soc.* **2004**, *126*, 13424.
(23) Paxton, W. F.; Sen, A.; Mallouk, T. E. *Chem.−Eur. J.* **2005**, *11*, 6462.
(24) Sanchez, S.; Ananth, A. N.; Fomin, V. M.; Viehrig, M.; Schmidt, O. G. *J. Am. Chem. Soc.* **2011**, *133*, 14860.
(25) Gao, W.; Sattayasamitsathit, S.; Orozco, J.; Wang, J. *J. Am. Chem. Soc.* **2011**, *133*, 11862.
(26) Wang, J.; Gao, W. *ACS Nano* **2012**, *6*, 5745.
(27) Solovev, A. A.; Mei, Y.; Ureña, E. B.; Huang, G.; Schmidt, O. G. *Small* **2009**, *14*, 1688.
(28) Zhao, G.; Pumera, M. *RSC Adv.* **2013**, *3*, 3963.
(29) Sanchez, S.; Solovev, A. A.; Mei, Y.; Schmidt, O. G. *J. Am. Chem. Soc.* **2010**, *132*, 13144.
(30) Mei, Y.; Huang, G.; Solovev, A. A.; Ureña, E. B.; Mönch, I.; Ding, F.; Reindl, T.; Fu, R. K. Y.; Chu, P. K.; Schmidt, O. G. *Adv. Mater.* **2008**, *20*, 4085.
(31) Manjare, M.; Yang, B.; Zhao, Y.-P. *Phys. Rev. Lett.* **2012**, *109*, 128305.
(32) Huang, W.; Manjare, M.; Zhao, Y. *J. Phys. Chem. C* **2013**, *117*, 21590.
(33) Howse, J. R.; Jones, R. A. L.; Ryan, A. J.; Gough, T.; Vafabakhsh, R.; Golestanian, R. *Phys. Rev. Lett.* **2007**, *99*, 048102.
(34) Baraban, L.; Makarov, D.; Streubel, R.; Mönch, I.; Grimm, D.; Sanchez, S.; Schmidt, O. G. *ACS Nano* **2012**, *6*, 3383.
(35) Baraban, L.; Tasinkevych, M.; Popescu, M. N.; Sanchez, S.; Dietrich, S.; Schmidt, O. G. *Soft Matter* **2012**, *8*, 48.
(36) Greenwood, N. N.; Earnshaw, A. *Chemistry of the Elements*; Pergamon Press: Oxford, 1997; pp 1218−1220.
(37) Dunderdale, G.; Ebbens, S.; Fairclough, P.; Howse, J. *Langmuir* **2012**, *28*, 10997.
(38) Wang, W.; Chiang, T.; Velegol, D.; Mallouk, T. E. *J. Am. Chem. Soc.* **2013**, *135*, 10557.
(39) Zhao, G.; Sanchez, S.; Schmidt, O. G.; Pumera, M. *Nanoscale* **2013**, *5*, 2909.
(40) Mou, F.; Chen, C.; Ma, H.; Yin, Y.; Wu, Q.; Guan, J. *Angew. Chem., Int. Ed.* **2013**, *52*, 7208.
(41) Gao, W.; Pei, A.; Wang, J. *ACS Nano* **2012**, *6*, 8432.